Biochimica et Biophysica Acta 1857 (2016) 350–358

Contents lists available at ScienceDirect

Biochimica et Biophysica Acta

journal homepage: www.elsevier.com/locate/bbabio

cAMP regulates the functional activity, coupling efficiency and structural organization of mammalian F_OF_1 ATP synthase

Domenico De Rasmo [a,*], Loris Micelli [b], Arcangela Santeramo [b], Anna Signorile [b], Paolo Lattanzio [a], Sergio Papa [a,b]

[a] Institute of Biomembrane and Bioenergetics, National Research Council, Bari 70124, Italy
[b] Department of Basic Medical Sciences, Neurosciences and Sense Organs, University of Bari "Aldo Moro", Bari 70124, Italy

ARTICLE INFO

Article history:
Received 7 August 2015
Received in revised form 30 December 2015
Accepted 5 January 2016
Available online 13 January 2016

Keywords:
Mitochondria
F_OF_1 ATP synthase
Intramitochondrial cAMP
sAC

ABSTRACT

The present study shows that in isolated mitochondria and myoblast cultures depletion of cAMP, induced by sAC inhibition, depresses both ATP synthesis and hydrolysis by the F_OF_1 ATP synthase (complex V) of the oxidative phosphorylation system (OXPHOS). These effects are accompanied by the decrease of the respiratory membrane potential, decreased level of F_OF_1 connecting subunits and depressed oligomerization of the complex. All these effects of sAC inhibition are prevented by the addition of the membrane-permeant 8-Br-cAMP. These results show, for the first time, that cAMP promotes ATP production by complex V and prevents, at the same time, its detour to a mitochondrial membrane leak conductance, which is involved in cell death.

1. Introduction

In mammalian cells cAMP can be produced by the transmembrane adenylyl cyclase (tmAC) or by the soluble cyclase (sAC) and degraded to 5′-AMP by phosphodiesterases [1,2]. cAMP released in the cytosol by tmAC, acts as second messenger in response to the binding to specific receptors of extracellular signal molecules, like hormones and neurotransmitters (cAMP cascade), and activates different processes interacting with independent cAMP signaling microdomains [2,3]. sAC, widely expressed in different subcellular compartments, including cytosol, nuclei, mitochondria *etc.*, activated by bicarbonate [4] and Ca^{2+}. [5,6], amplifies the regulatory effects of cAMP, it is to say that sAC provides an additional dimension to the signaling activity of cAMP, which can be degraded by specific phosphodiesterases in the same compartment where it is produced by adenylyl cyclases [2,7]. In mitochondria cAMP can interact with separate microdomains localized both on the outer mitochondrial membrane [8] and in the mitochondrial matrix [9], being the inner mitochondrial membrane impermeable to cytosolic cAMP [6]. Work from different laboratories has shown that both the cAMP produced outside [10,11] and that produced inside mitochondria [2,12,13] play a critical role in the regulation of functional activity of respiratory chain complex I [10,11] and complex IV [2,13], mitochondrial biogenesis [14], mitochondrial dynamics [15], mitochondrial free radical balance [16] and human diseases [14,17]. Contribution from our laboratory has characterized the role of the cAMP/PKA (cAMP dependent protein kinase) system in the regulation of functional activity [11] and turnover [18] of complex I and the role of its dysfunction in neurodegenerative disorders [14]. In particular, it has been found that, cytosolic cAMP produced by tmAC, in response to extracellular signal molecules (cAMP cascade), has an impact on complex I [11,13].

We have now studied in isolated rat-liver mitochondria and rat-heart myoblasts the impact of cAMP on the functional activity and structural organization of the mitochondrial F_OF_1 ATP synthase (complex V) of the oxidative phosphorylation system (OXPHOS).

In mammalian mitochondria complex V is composed of 18 different subunits assembled in three sectors, the F_1 extrinsic catalytic sector, the F_O membrane, proton translocating sector and the F_1–F_O connecting stalk [19,20]. Eight different subunits 3 α, 3 β, 1 γ, 1 δ and 1 ε of F_1 and 1 a, 1 b, 10–12 c subunits of F_O are conserved from prokaryotes to eukaryotes, all the others are supernumerary subunits of the eukaryotic complex. Subunits c, γ, δ and ε constitute a rotor element, whose $\Delta\mu H^+$ driven motion, within a stator element composed of F_1-α, F1-β, F_O-a and some of the supernumerary subunits, support ATP synthesis at the catalytic α/β site [21]. ATP hydrolysis drives motion of the rotor, in the opposite direction of ATP synthesis, with generation of $\Delta\mu H^+$ [21,22]. In yeast and mammalian mitochondria complex V exists in

Abbreviations: 8-Br-cAMP, 8-Bromoadenosine 3′,5′-cyclic monophosphate; KH7, (E)-2-(1H-Benzo[d]imidazol-2-ylthio)-N′-(5-bromo-2-hydroxybenzylidene)propanehydrazide; CAI, carbonic anhydrase inhibitor; PKA, cAMP dependent protein kinase; PKI, protein kinase inhibitor; mPTP, mitochondrial permeability transition pore; RLM, rat liver mitochondria; sAC, soluble adenylyl cyclase; tmAC, transmembrane adenylyl cyclase.

* Corresponding author at: Institute of Biomembrane and Bioenergetics, National Research Council (CNR), 70126 Bari Italy, at Department of Basic Medical Sciences, Neurosciences and Sense Organs, University of Bari "Aldo Moro", Policlinico, P.zza G. Cesare, 11, 70124 Bari, Italy.
E-mail address: d.derasmo@ibbe.cnr.it (D. De Rasmo).

http://dx.doi.org/10.1016/j.bbabio.2016.01.006
0005-2728/

monomeric, dimeric and oligomeric states [20,23–25]. Complex V oligomerization appears to determine the cristae organization of the inner mitochondrial membrane [26] thus optimizing energy coupling [27,28]. Impairment of the structural and functional organization of the ATP synthase complex results in a membrane leak [27,29], apparently involving subunit c [30,31]. There is evidence that this leak represents an essential component of the mitochondrial permeability transition pore (mPTP) [30,31], which is involved in cell death [32].

The results of the present work on isolated rat-liver mitochondria (RLM) and rat-heart myoblast cultures show that cAMP regulates the ATP hydrolytic and synthase activities, coupling efficiency, oligomerization and stability of some stalk subunits of the F_OF_1 ATP synthase.

2. Materials and methods

2.1. Isolation of mitochondria and treatments

Rat liver mitochondria (RLM) were isolated by differential centrifugation as described in [33]. After isolation, mitochondria were incubated for 10 min at 30 °C in 10 mM Tris–HCl, pH 7.4; 25 mM sucrose; 75 mM sorbitol; 100 mM KCl; 10 mM K_2HPO_4; 0.05 mM EDTA; 5 mM $MgCl_2$; 1 mg/ml BSA. Further conditions are specified in the legends to figures.

2.2. Cell cultures and treatments

Rat heart myoblasts (H9c2, A.T.T.C. #CRL1446) were grown in the exponential phase in high glucose Dulbecco's modified Eagle's medium (DMEM, EuroClone) supplemented with 10% fetal bovine serum (FBS), plus 2 mM glutamine (Euroclone), 100 IU/ml penicillin (Euroclone) and 100 IU/ml streptomycin (Euroclone) at 37 °C. Further conditions are specified in the legends to figures.

2.3. cAMP assay

cAMP level was measured in RLM samples using a direct immunoassay kit (Assay Designs, Ann Arbor, Michigan, USA) as described by the manufacturer. Briefly, after incubation RLM were pelleted by centrifugation and resuspended in 0.1 N HCl, centrifuged 1000 ×*g*, for 10 min and the supernatant used for cAMP determination. Total protein concentration was determined by Bio-Rad protein assay. For cAMP assay in the cultured cells, the medium was aspirated and 1 ml of 0.1 M HCl was added to the cell layer followed by 10 min incubation at 37 °C. The lysed cells were scraped into Eppendorf tubes. The samples were centrifuged at 1300 ×*g* for 10 min at 4 °C. The supernatants were used to determine cAMP concentration using a direct immunoassay kit (Assay Designs) as described by the manufacturer. Total protein concentration was determined by Bio Rad protein assay. The cAMP levels in the samples were normalized to the protein concentration and expressed as pmol/mg protein.

2.4. Measurement of activities of the respiratory chain complexes

RLM were frozen and thawed three times to allow complete accessibility of substrates to the enzymes.

Harvested myoblasts were exposed to ultrasound energy for 15 s at 0 °C. After exposure to ultrasounds, the cellular lysate was centrifuged at 500 ×*g* for 5 min at 4 °C and the supernatant recovered and centrifuged at 20,000 ×*g* for 5 min at 4 °C. The pellet was used for the determinations.

The NADH-UQ oxidoreductase (complex I), succinate-cytochrome *c* oxidoreductase (complex II + III) and cytochrome c oxidase (complex IV) activities were performed as described in [18].

2.5. Measurement of F_OF_1 ATPase activity

ATP hydrolase activity was measured by an ATP-regenerating system. Frozen and thawed RLM or myoblasts cells were suspended (at 0.1 mg protein/ml) in a buffer consisting of 375 mM sucrose, 75 mM KCl, 30 mM Tris–HCl pH 7.4, 3 mM $MgCl_2$, 2 mM PEP, 55 U/ml lactate dehydrogenase, 40 U/ml pyruvate kinase, 0.3 mM NADH. The reaction was started by the addition of 1 mM ATP and the oxidation of NADH was followed at 340 nm.

2.6. Measurement of mitochondrial ATP production

RLM were suspended at 0.2 mg protein/ml in 75 mM sucrose, 50 mM KCl, 30 mM TRIS, 2 mM KH_2PO_4, 10 mM EGTA, pH 7.4, supplemented with 10 mM succinate, 0.3 mM ADP and 0.3 mM P1,P5-di(adenosine-5′) pentaphosphate (Ap5A) in the presence or in the absence of 2 μg/mg protein of oligomycin. After five minute incubation at 30 °C, mitochondrial ATP was measured using a luciferin–luciferase reaction system (PROMEGA, Madison, Wisconsin, USA).

2.7. Measurement of membrane potential

The mitochondrial membrane potential ($\Delta\psi$) in RLM was measured following the safranin-O fluorescence quenching at 525 nm (excitation), 575 nm (emission) with a Jasco FP 6200 spectrofluorimeter. RLM (0.25 mg/ml) were suspended in 1 ml of 75 mM sucrose, 50 mM KCl, 30 mM Tris–HCl, (pH 7.4), 2 mM KH_2PO_4, 2 mM $MgCl_2$ and 10 μM EGTA, supplemented with 5 μM safranin-O, at 25 °C. $\Delta\psi$ was generated by the addition of 10 mM succinate (in the presence of 2 μg/ml rotenone) or by the addition of 1.5 mM ATP. Other details are specified in the legend to Fig. 3. The mitochondrial membrane potential in myoblasts was measured using a laser scanning confocal microscope analysis (LSCM) (Leica TCS SP8 microscope; images were collected using a 60× objective) on cells seeded onto fibronectin-coated glass-bottom dishes. The living cells were incubated for 15 min with 0.3 μM MitoTracker probe (554 nm excitation and 576 nm emission wavelength), washed with Krebs' buffered salt solution (20 mM Hepes, pH 7.4, 135 mM NaCl, 5 mM KCl, 0.4 mM KH_2PO_4, 1 mM $MgSO_4$, 0.1% w/v glucose, 1 mM $CaCl_2$), and examined by LSCM. The red fluorescence intensity of MitoTracker was analyzed by exciting the sample with a solid state laser 552 nm. Acquisition, storage, and data analysis were done using Leica software.

2.8. Measurement of oxygen consumption rate

The respiratory activity of liver mitochondria was measured polarographically with a Clark-type electrode, in an all-glass reaction chamber magnetically stirred, at 30 °C. RLM, suspended at a final concentration of 0.25 mg/ml, or 10^6 myoblast cells were resuspended in 75 mM sucrose, 50 mM KCl, 30 mM Tris–HCl, (pH 7.4), 2 mM KH_2PO_4, 2 mM $MgCl_2$ and 10 μM EGTA. State IV respiration was started by the addition of 10 mM succinate in the presence of 2 μg/ml rotenone. State III and uncoupled respiration were obtained by adding ADP (0.5 mM) and CCCP (0.25 μM), respectively. For measurement of OXPHOS efficiency (P/O ratios), succinate-dependent respiration was stimulated transiently by the addition of 0.08 mM ADP. 0.3 mM P1,P5-di(adenosine-5′) pentaphosphate (Ap5A) was added to prevent dissipation of ADP by adenylate kinase. The P/O was calculated as the ratio between the amount (nano-moles) of added ADP and the oxygen (natoms) consumed during the ADP-induced state 3 respiration.

2.9. Electrophoretic procedures and Western blotting

RLM were isolated and treated as described before. Myoblasts were harvested from Petri dishes with 0.05% trypsin, 0.02% EDTA, pelleted by centrifugation at 500 ×*g* and then resuspended in phosphate-

buffered saline, pH 7.4 (PBS). For SDS-PAGE, RLM and myoblasts suspensions were resuspended in lysis buffer at final concentration of 2 mg/ml, loaded on 8% polyacrylamide gel, transferred to a nitrocellulose membrane and immunoblotted with the antibodies described in Fig. 5. Densitometric analysis was performed by VersaDoc imaging system (BioRad, Milan, Italy) using QuantityOne software (BioRad). The supramolecular organization of the ATP synthase was evaluated by CN-PAGE. For RLM, 500 mg of mitochondrial proteins was pelleted by centrifugation for 10 min at 12,000 ×*g* at 4 °C. The pellet was solubilized at 10 mg/ml in extraction buffer (150 mM potassium acetate, 12% glycerol (w/v), 2 mM 6-aminocaproic acid, 1 mM disodic EDTA, 30 mM HEPES pH 7.4) supplemented with digitonin (3.5 mg/mg mitochondrial protein). After 20 min on ice, mitochondrial extracts were centrifuged for 30 min at 20,000 ×*g* at 4 °C. Supernatants were supplemented with 36 mM 6-aminocaproic acid and loaded onto polyacrylamide gradient (3–13%) gel. CN-PAGE as in [34]. For myoblasts, the harvested cells were resuspended in PBS and treated with digitonin (2 mg/mg cellular protein), for 10 min on ice, and then centrifuged for 10 min at 10,000 ×*g* at 4 °C. The recovered pellet, enriched in mitochondria, was resuspended in extraction buffer supplemented with digitonin (9 mg/mg protein) for 15 min on ice, and then centrifuged for 20 min at 20,000 ×*g* at 4 °C. Supernatants were loaded onto polyacrylamide gradient (3–13%) gel.

2.10. In-gel ATPase activity

After electrophoresis the gels were incubated at room temperature in 35 mM Tris–HCl pH 7.4, 270 mM glycine, 14 mM MgSO4, 0.2% (w/v) $Pb(NO_3)_2$ and 8.0 mM ATP. ATPase activity was revealed by a white precipitate on the gel of lead phosphate [35]. Densitometric analysis was performed by VersaDoc imaging system.

2.11. Animal care

All experiments were performed in accordance with national and institutional guidelines for animal welfare, adhering to protocols approved by the institutional committee on research animal care. A written confirmation of authorization was obtained from local authority (n. 60895-X10, Comitato Etico per la Sperimentazione Animale, Area Sicurezza sul Lavoro, Dipartimento Amministrativo per la Sanità, University of Bari).

3. Results

3.1. Effect of cAMP on the activity of OXPHOS complexes in RLM and myoblast cultures

Analysis of the mitochondrial cAMP level in RLM shows that, under the experimental conditions used, RLM treatment with 50 μM KH7, an inhibitor of sAC [12], reduced significantly the cAMP level (Fig. 1A) (see also ref. [18]). RLM treatment with acetazolamide, a carbonic anhydrase inhibitor (CAI) which indirectly inhibits sAC [12,36], also reduced the mitochondrial cAMP level (see also [12 and 37]) (Fig. 1A). CAI treatment of myoblast cultures reduced the cAMP content of the myoblast lysate (Fig. 1B). It can be noted that whilst in RLM, increase of CAI concentration from 1 to 100 μM did not reduce further the cAMP mitochondrial level, in myoblast cultures, the reduction of cAMP content increased as the CAI concentration was raised up to 50 μM, but it was not that extensive as that caused in RLM. Thus the additional experiments on the effects of CAI were carried out at 1 μM for RLM and 50 μM for myoblast cultures.

KH7 or CAI treatment of RLM, which depressed the activity of complex IV (see [12]) caused also inhibition of the ATP hydrolase activity (Fig. 2). Both these effects were reversed by the addition of the membrane-permeant cAMP analog, 8-Br-cAMP, but not by the addition of membrane-impermeant cAMP (Fig. 2). It can be noted that specific inhibitors of PKA, like the permeant inhibitory peptide PKI (protein kinase inhibitor) and the competitive inhibitor H89, had no effect on the ATP hydrolase activity of control RLM, neither did these inhibitors prevent the rescue effect exerted by 8-Br-cAMP on the KH7 depressed ATP hydrolase activity (see inset of Fig. 2). Treatment of myoblast

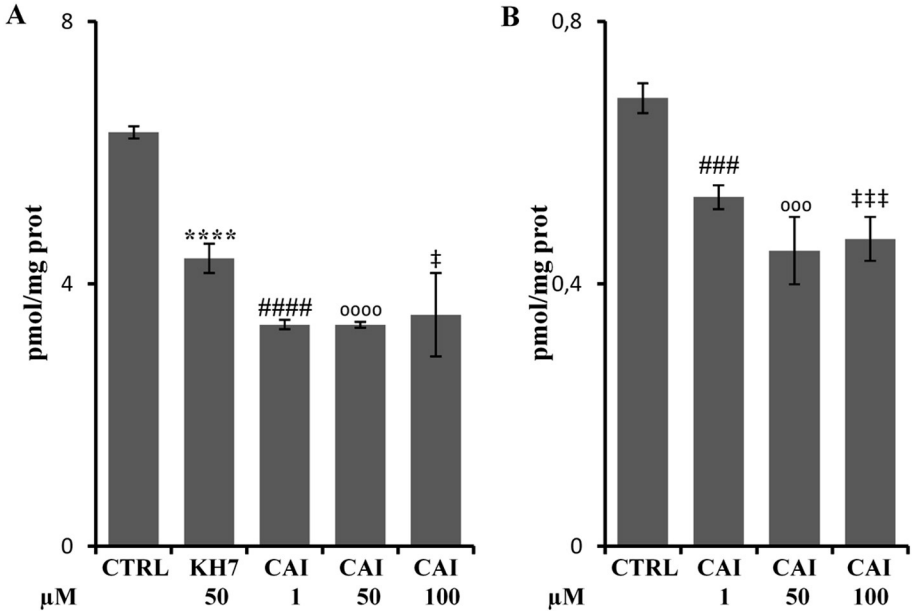

Fig. 1. KH7 and CAI lower the cAMP level in RLM and myoblast cultures. Panel A, RLM were treated for 10 min at 30 °C in the absence (CTRL) or in the presence of 50 μM KH7 or CAI (1 μM, 50 μM or 100 μM). Panel B, myoblast cultures were treated for 30 min in the absence (CTRL) or in the presence of CAI 1 μM, 50 μM or 100 μM. The histograms represent the mean values of duplicate determinations of cAMP level in three separate RLM preparations (panel A) or myoblast cultures (panel B), expressed as pmoles per mg protein. Error bars indicate standard deviations.$^{****}p < 0.001$: KH7 *vs* CTRL; $^{\#\#\#\#}p < 0.001$, $^{\#\#\#}p < 0.005$: 1 μM CAI *vs* CTRL; $^{oooo}p < 0.001$, $^{ooo}p < 0.005$: 50 μM CAI *vs* CTRL; $^{‡‡‡}p < 0.005$, $^{‡}p < 0.05$: 100 μM CAI *vs* CTRL. Student's t test. For other experimental details see under Materials and methods.

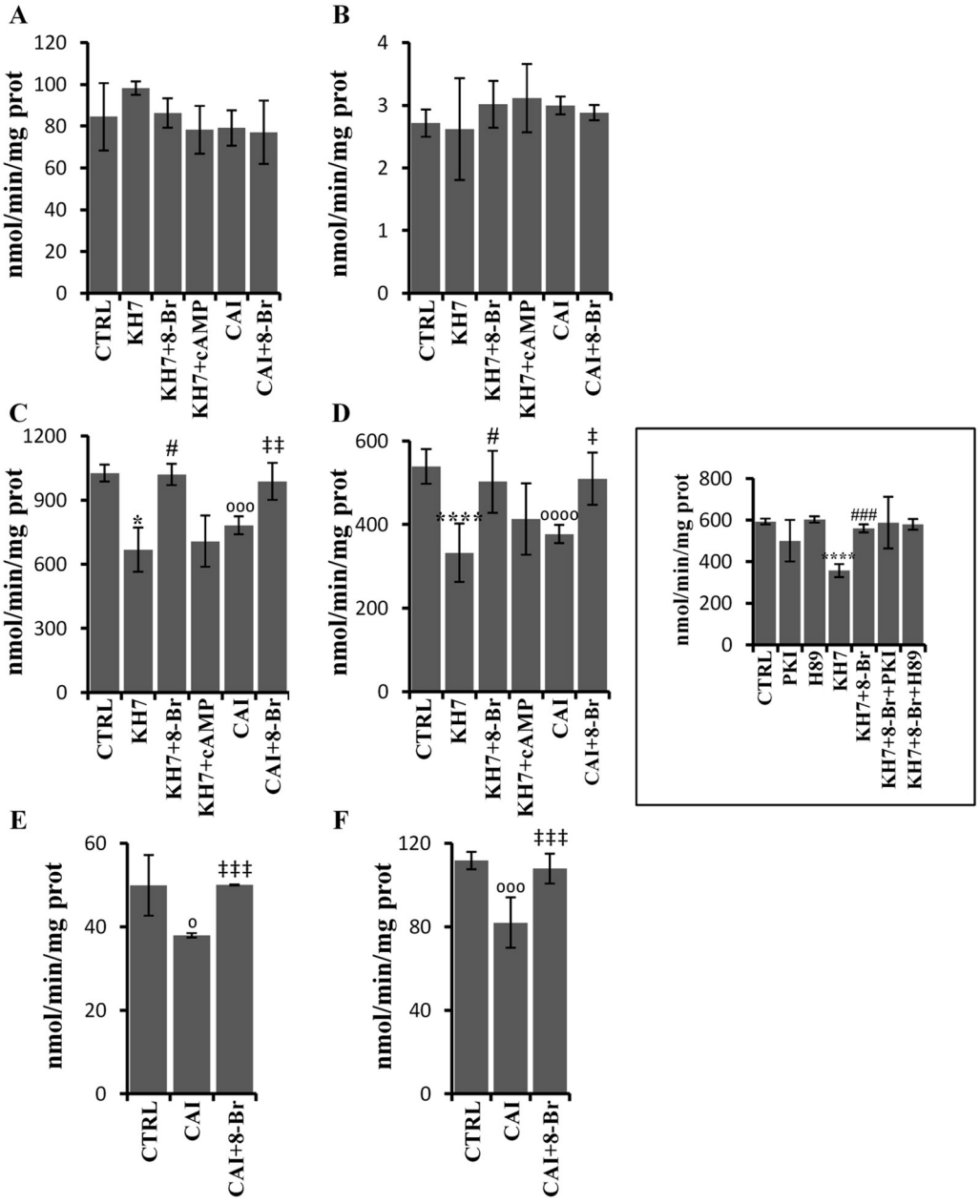

Fig. 2. Effects of KH7, CAI and cAMP on respiratory chain complexes and ATP hydrolase activities in RLM and myoblast cultures. Panels A–D, RLM were treated for 10 min at 30 °C in the absence (CTRL) or in the presence where indicated of 50 μM KH7 (KH7), KH7 plus 100 μM 8-Br-cAMP (KH7 + 8-Br), KH7 plus 100 μM cAMP (KH7 + cAMP), 1 μM CAI (CAI) or CAI plus 100 μM 8-Br-cAMP (CAI + 8-Br). Panels E–F, myoblast cultures were treated for 30 min in the absence (CTRL) or in the presence of 50 μM CAI (CAI) or CAI plus 100 μM 8-Br-cAMP (CAI + 8-Br). After incubation, the activities of NADH:ubiquinone oxidoreductase (panel A), complex II + III (panel B), cytochrome c oxidase (panels C and E) and ATP hydrolase (panels D and F) were determined as described under Materials and methods. Inset, ATP hydrolase activity in RLM treated for 10 min at 30 °C in the absence (CTRL) or in the presence 1 μM permeant PKI (PKI), 5 μM H89 (H89), of KH7 (KH7), KH7 plus 8-Br-cAMP (KH7 + 8-Br), KH7 plus 8-Br-cAMP and PKI (KH7 + 8-Br + PKI) and KH7 plus 8-Br-cAMP and H89 (KH7 + 8-Br + H89). The histograms represent the mean values of duplicate determinations in three separate RLM preparations (panels A–D) or myoblast cultures (panels E–F). Errors bars indicate standard deviations. ****$p < 0.001$,*$p < 0.05$: KH7 *vs* CTRL; ###$p < 0.005$, #$p < 0.05$: KH7 + 8-Br-cAMP *vs* KH7; °°°$p < 0.005$, °$p < 0.05$: CAI *vs* CTRL; ‡‡‡$p < 0.005$, ‡‡$p < 0.01$, ‡$p < 0.05$: CAI + 8-Br-cAMP *vs* CAI. Student's t test. For experimental details see under Materials and methods and legend to Fig. 1.

cultures with CAI also depressed the activities of complex IV (see [12]) and ATP hydrolase (Fig. 2), both effects being reversed by the addition of 8-Br-cAMP (Fig. 2). In isolated RLM no effect of KH7, CAI or 8-Br-cAMP was, under the prevailing conditions used, observed on the specific activities of complex I and complex II + III (Fig. 2).

3.2. cAMP preserves the mitochondrial membrane potential

Fig. 3 shows the effects of KH7, CAI and 8-Br-cAMP on the mitochondrial membrane potential monitored by quenching of safranin fluorescence in RLM and the effects of CAI and 8-Br-cAMP on the mitochondrial membrane potential in myoblast cultures, monitored by confocal microscopy using the MitoTracker probe. KH7 or CAI treatment of RLM caused a reduction in the extent of the mitochondrial membrane potential, generated by succinate used as respiratory substrate (Fig. 3A and B). The depressing effect of KH7 and CAI was prevented by the concomitant presence of 8-Br-cAMP. The ADP induced drop of the mitochondrial membrane potential, which was abolished by oligomycin, the inhibitor of the ATP synthase (Fig. 3B), was depressed by RLM treatment with KH7 or CAI and restored by 8-Br-cAMP (Fig. 3A). The traces in

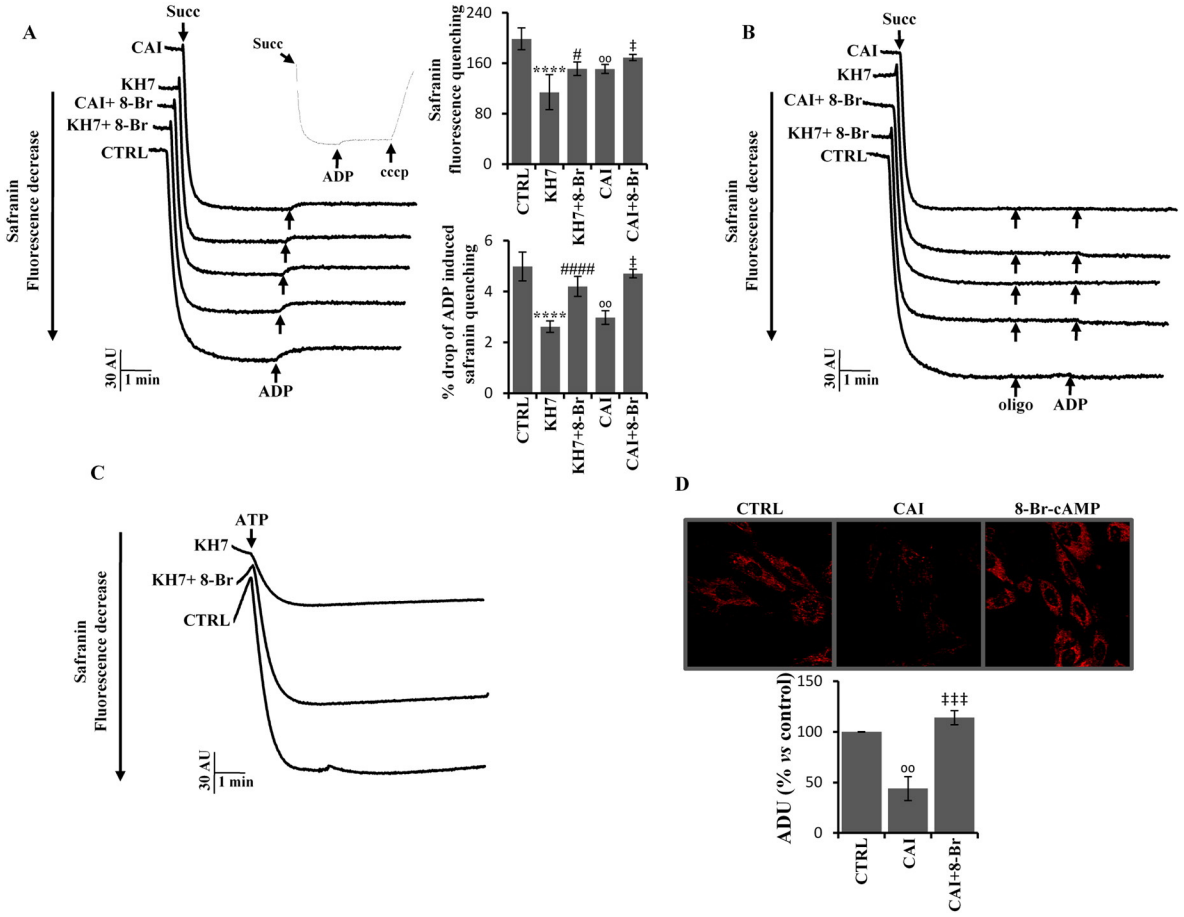

Fig. 3. KH7 and CAI impair and 8-Br-cAMP rescues the mitochondrial membrane potential in RLM and myoblast cultures. Panels A–C, RLM were treated for 10 min at 30 °C in the absence (CTRL) or in the presence, where indicated, of KH7 (KH7), KH7 plus 8-Br-cAMP (KH7 + 8-Br), CAI (CAI) or CAI plus 8-Br-cAMP (CAI + 8-Br). The mitochondrial membrane potential (Δψ) was monitored following the safranin-O fluorescence quenching. Panels A and B, Δψ was generated by the addition of 10 mM succinate to RLM. Where indicated 0.3 mM ADP was added, in the absence or presence of 2 μg/ml oligomycin. Δψ dissipation by 0.25 μM CCCP addition is shown in the inset. The histograms represent the mean values of duplicate determinations in three separate RLM preparations of the extent of succinate-supported Δψ and the ADP-dependent drop of Δψ expressed as percentage of the proper extent of succinate-dependent Δψ. Errors bars indicate standard deviations. Panel C, Δψ was generated in RLM by the addition of 1.5 mM ATP to RLM. Panel D, LSCM of mitochondrial membrane potential detected by red fluorescence of MitoTracker probe in myoblast cultures treated for 30 min in the absence (CTRL) or in the presence of 50 μM CAI (CAI) or CAI plus 8-Br-cAMP (CAI + 8-Br). The intensity of fluorescence is expressed in arbitrary densitometric units (ADU) as percentage changes with respect to control. The histograms represent the mean values of determinations in three separate myoblast cultures preparations. Errors bars indicate standard deviations. $^{****}p < 0.001$: KH7 *vs* CTRL; $^{\#\#\#\#}p < 0.001$, $^{\#}p < 0.05$: KH7 + 8-Br-cAMP *vs* KH7; $^{oo}p < 0.01$: CAI *vs* CTRL; $^{‡‡‡}p < 0.005$, $^{‡}p < 0.05$: CAI + 8-Br-cAMP *vs* CAI. Student's t test. For experimental details see under Materials and methods and legend to Figs. 1 and 2.

Fig. 3C show that KH7 caused a decrease in the extent of the membrane potential generated by ATP hydrolysis, an effect which was also prevented by 8-Br-cAMP. Laser scanning confocal microscopy showed that treatment of myoblast cultures with 50 μM CAI resulted in a decrease of the mitochondrial membrane potential, which was reversed by the addition of 8-Br-cAMP (Fig. 3D).

In RLM, KH7 treatment exerted a stimulatory effect on succinate supported respiration both in state IV and ADP induced state III. CAI treatment exerted a stimulatory effect only in state IV (Fig. 4A and B). These effects of KH7 and CAI were prevented by 8-Br-cAMP. No change was observed in CCCP-stimulated succinate respiration (Fig. 4C). KH7 treatment of RLM resulted in a drop of the P/O ratio (Fig. 4D) and in the oligomycin sensitive ATP production (Fig. 4E), both effects being counteracted by the addition of 8-Br-cAMP. The stimulatory effect of CAI on succinate supported respiration in state IV, as well as the CAI induced drop of the P/O ratio, was also observed in myoblast cultures (Fig. 4F and I), both effects being reversed by the addition of 8-Br-cAMP (Fig. 4F and I). Also in myoblast cultures no change was caused by CAI on succinate supported respiration in the ADP induced state III and CCCP-stimulated respiration (Fig. 4G and H).

3.3. cAMP preserves the level of ATP synthase subunits and its supramolecular organization

The effect of KH7 and CAI on the amount of the ATP synthase subunits in RLM was analyzed by SDS-PAGE of the mitochondrial proteins and immunoblotting with specific antibodies. The contents of α, β and IF1 subunits were unaffected by KH7 or CAI treatment of RLM (Fig. 5A). The contents of OSCP, d and ATP6 subunits of the stator of the complex were, instead, reduced in KH7 and CAI treated RLM and rescued by the concomitant presence of 8-Br-cAMP (Fig. 5A). In CAI treated myoblast cultures reduced levels of OSCP, d and ATP6 subunits of ATP synthase were observed, all rescued by 8-Br-cAMP. No change was caused by CAI in the content of α, β and IF1 subunits (Fig. 5B).

Since a specific reduction of the stator element of ATP synthase has been associated with alteration of its supramolecular organization [28], the ATP synthase oligomerization state was analyzed by separation of protein complexes in clear-native polyacrylamide gel electrophoresis (CN-PAGE). The in-gel ATPase activity of untreated RLM, revealed more bands (Fig. 6A and B). These bands can be attributed to the monomeric, dimeric and oligomeric forms of ATP synthase. The treatment of RLM with KH7 resulted in a decrease of the oligomeric form of the complex

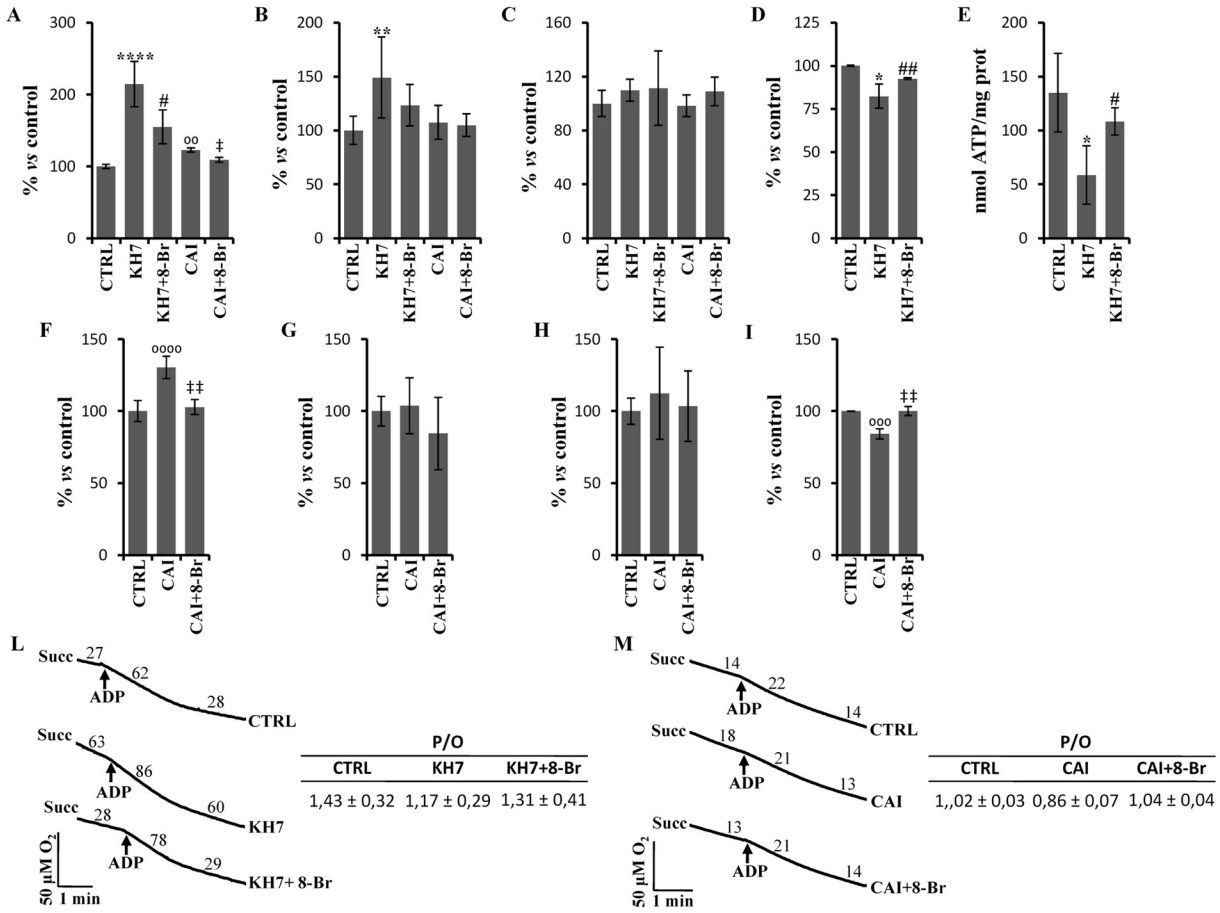

Fig. 4. KH7 and CAI affect the respiratory rate, P/O and ATP production in RLM and myoblast cultures. Panels A–E, RLM were treated for 10 min at 30 °C in the absence (CTRL) or in the presence, where indicated, of KH7 (KH7), KH7 plus 8-Br-cAMP (KH7 + 8-Br), CAI (CAI) or CAI plus 8-Br-cAMP (CAI + 8-Br) as described in the figure. Panels F–I, myoblast cultures treated for 30 min in the absence (CTRL) or in the presence of CAI (CAI) or CAI plus 8-Br-cAMP (CAI + 8-Br). Panels A and F, oxygen consumption in RLM and myoblasts, respectively, supplemented with 10 mM succinate plus rotenone (state IV). Panels B and G, oxygen consumption in RLM and myoblasts supplemented with succinate and 0.5 mM ADP (state III). Panels C and H, oxygen consumption in RLM and myoblasts supplemented with 0.25 µM CCCP. Panels D and I, measurement of OXPHOS efficiency (P/O ratios) in succinate-dependent respiration stimulated transiently by the addition of 0.08 mM ADP. Panel E, succinate-dependent mitochondrial ATP production measured using a luciferin–luciferase reaction system in RLM. The histograms represent the mean values of duplicate determinations of the respiratory activity in three separate RLM preparations (panels A–E) or myoblast cultures (panels F–I). In panels A–D (RLM) and F–I (myoblasts) the activities, measured in the presence of the various effectors, are expressed as % changes with respect to control. Errors bars indicate standard deviations. $^{****}p < 0.001$, $^{**}p < 0.01$, $^{*}p < 0.05$: KH7 *vs* CTRL; $^{\#\#}p < 0.01$, $^{\#}p < 0.05$: KH7 + 8-Br-cAMP *vs* KH7; $^{oooo}p < 0.001$, $^{ooo}p < 0.005$: CAI *vs* CTRL; $^{\ddagger\ddagger}p < 0.01$: CAI + 8-Br-cAMP *vs* CAI. Student's t test. Panels L and M, traces of oxygen consumption in RLM and myoblast cultures, respectively, respiring with succinate. Numbers on the traces refer to the rate of oxygen consumption as nmol O_2 min^{-1} mg $protein^{-1}$ or 10^6 cells. The succinate-dependent respiration was followed by the addition of 0.08 mM ADP to induce transient stimulation of oxygen consumption. The table presents the means plus standard deviations of P/O values. For other experimental details see under Materials and methods and the legend to Figs. 1 and 2.

that was prevented by the concomitant addition of 8-Br-cAMP (Fig. 6A). In myoblast cultures CAI caused a reduction of the oligomeric band of ATP synthase which was prevented by 8-Br-cAMP (Fig. 6B). It has been shown that MG132 inhibits the activity of intramitochondrial protease(s) like Lon [18]. Treatment of RLM with MG132 prevented the decrease in the level of the ATP6, d and OSCP subunits, caused by KH7 (Fig. 7A), which was shown above to be counteracted by 8-Br-cAMP (Fig. 5A). The levels of KH7 insensitive β and α subunits of ATP synthase and IF1 were unaffected by MG132 (Fig. 7A). MG132 prevented, also, the KH7-induced depression of the ATP synthase oligomerization (Fig. 7B) and of the ATP hydrolase activity (Fig. 7C).

4. Discussion

The present study shows, for the first time, that cAMP regulates the catalytic activity, coupling efficiency and structural organization of the F_OF_1 ATP synthase in mammalian mitochondria. This represents a new regulatory attribute of the oxidative phosphorylation system (OXPHOS), that can have important implications in cellular physiology and human pathology.

cAMP production by sAC is promoted by bicarbonate and Ca^{2+} [2,4–6]. sAC activation by bicarbonate, with the consequent stimulation exerted by cAMP on the ATP synthase activity, can represent a positive response of the OXPHOS system to enhanced channeling to mitochondria of glycolytic pyruvate and its oxidative degradation to CO_2 in the citric-acid cycle [2,38]. In this way the utilization for ATP production of the free energy made available by pyruvate degradation can be optimized. sAC stimulation by Ca^{2+} [6], resulting in cAMP-mediated activation of the ATP synthase, can, on the other hand, represent a defense/compensatory mechanism against the depressing effect exerted by mitochondrial accumulation of Ca^{2+} on mitochondrial energy transduction and cell life.

The ATP synthase complex is a critical element of the overall OXPHOS system; the complex undergoes oligomerization in the inner mitochondrial membrane [23–25]. Oligomerization of the ATP synthase complex is involved in the formation of cristae of the inner

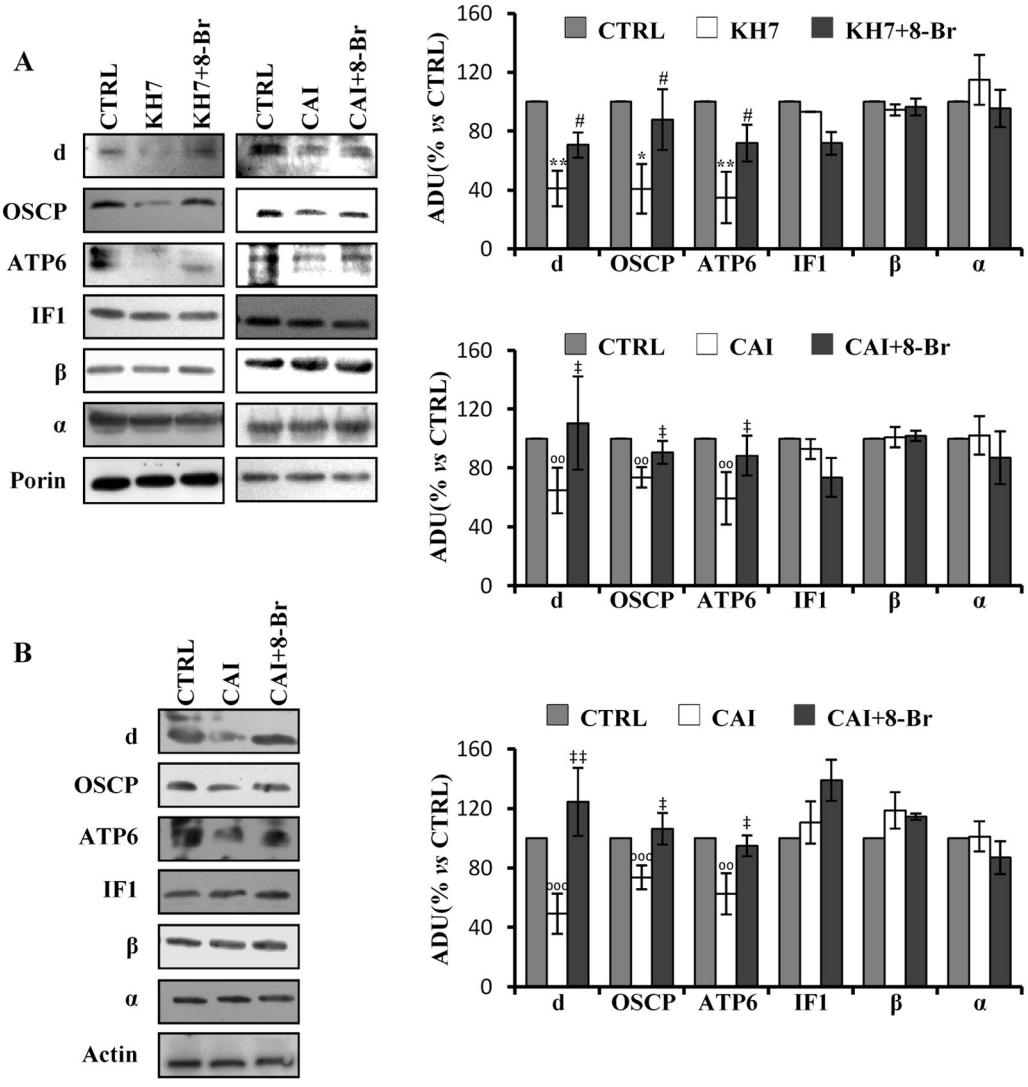

Fig. 5. Effects of KH7, CAI and 8-Br-cAMP on the level of subunits of the ATP synthase complex in RLM and myoblast cultures. Panel A, RLM were treated for 10 min at 30 °C in the absence (CTRL) or in the presence, where indicated, of KH7 (KH7), KH7 plus 8-Br-cAMP (KH7 + 8-Br), CAI (CAI) or CAI plus 8-Br-cAMP (CAI + 8-Br) as described in the figure. Panel B, myoblast cultures treated for 30 min in the absence (CTRL) or in the presence of CAI (CAI) or CAI plus 8-Br-cAMP (CAI + 8-Br). After incubation, RLM proteins (panel A) or myoblast cellular proteins (panel B) were loaded on 8% SDS-PAGE, transferred to nitrocellulose membranes and immunoblotted with the antibodies against the subunits specified in the figure. Protein loading was assessed by reprobing the blots with the porin antibody (panel A) or actin (panel B). The histograms represent the percentage of ADU changes with respect to the ADU of control untreated RLM (panel A) or myoblast cultures (panel B). The values are means ± standard deviation of determinations in three separate RLM preparations (panel A) or myoblast cultures (panel B). $^{**}p < 0.01$, $^{*}p < 0.05$: KH7 *vs* CTRL; $^{\#}p < 0.05$: KH7 + 8-Br-cAMP *vs* KH7; $^{ooo}p < 0.005$, $^{oo}p < 0.01$: CAI *vs* CTRL; $^{\ddagger\ddagger}p < 0.01$, $^{\ddagger}p < 0.05$: CAI + 8-Br-cAMP *vs* CAI. Student's t test. For experimental details see under Materials and methods and legend to Figs. 1 and 2.

mitochondrial membrane [26], which constitute a localized microenvironment with high capacity to maintain and utilize for ATP synthesis the respiratory membrane potential [27,28].

Our results show that depletion of cAMP in RLM or in myoblast cultures, caused by sAC inhibition by KH7 or CAI, depressed both ATP synthesis, driven by the membrane potential, with a decrease of the P/O ratio, and the membrane potential generating ATP hydrolysis.

Interesting enough the regulatory effect of cAMP on the enzymatic activity of the ATP synthase, was accompanied, both in RLM and myoblast cultures, by positive cAMP impact on the oligomerization of the complex and conservation of the respiratory mitochondrial membrane potential. Also these activities were depressed by KH7 or CAI, and rescued by the addition of 8-Br-cAMP. KH7 or CAI treatment of RLM or myoblast cultures resulted in a decreased level of OSCP, ATP6 and d subunits of the stator of the ATP synthase, that was prevented by added 8-Br-cAMP. A secondary uncoupling action of KH7 could contribute to the effect of KH7. This isn't, however, the case of CAI. Furthermore it can be noted that all the inhibitory effects of KH7 and CAI were both equally reversed by 8-Br-cAMP. The present results, taken together, indicate that depletion of cAMP causes destabilization of the stator of the complex and functional F_1–F_O connection, thus resulting in a membrane leak. A leak in the ATP synthase is proposed to represent a component of the mitochondrial permeability transition pore (mPTP) [29–31].

The prevention of the KH7 depressing effect on ATP synthase subunits by MG132 (Fig. 7), which is known to inhibit the mitochondrial Lon protease [18], suggests that this enzyme could be involved in the degradation of the ATP synthase subunits. As shown in the inset of Fig. 2, specific inhibitors of PKA, like PKI and H89, had no effect on the ATP hydrolase activity of control RLM neither did these inhibitors prevent the rescue effect exerted by 8-Br-cAMP on the KH7 depressed ATP hydrolase activity. This would exclude a direct role of intramitochondrial PKA [9] in the cAMP effects described in the present work. The possibility that other cAMP dependent downstream effectors

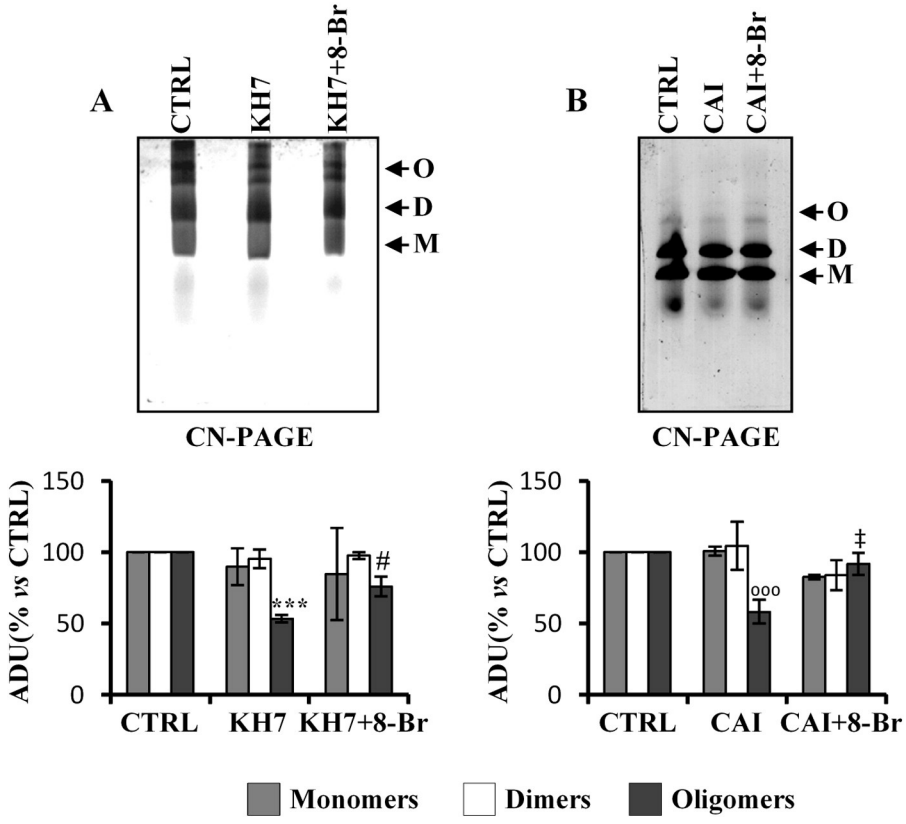

Fig. 6. Effects of KH7, CAI and 8-Br-cAMP on the supramolecular organization of the ATP synthase complex in RLM and myoblast cultures. Panel A, RLM were treated for 10 min at 30 °C in the absence (CTRL) or in the presence, where indicated, of KH7 (KH7) or KH7 plus 8-Br-cAMP (KH7 + 8-Br). Panel B, myoblast cultures treated for 30 min in the absence (CTRL) or in the presence of CAI (CAI) or CAI plus 8-Br-cAMP (CAI + 8-Br). Rat liver mitochondrial proteins or proteins of the mitochondrial enriched fraction of myoblasts cells were solubilized with digitonin (3.5 mg/mg mitochondrial protein and 9 mg/mg cellular protein, respectively). Mitochondrial complexes were separated by CN-PAGE and the gels incubated with ATP and lead nitrate to reveal the ATPase activity as described under Materials and methods. (M: monomer; D: dimer; O: oligomer). The figures, in inverted colors, are representative of three independent experiments. The histograms represent the ADU percentage changes with respect to the ADU of control untreated RLM (panel A) or myoblast cultures (panel B). The values are means ± standard deviation of determinations in three separate RLM preparations (panel A) or myoblast cultures (panel B). $^{***}p < 0.005$: KH7 *vs* CTRL; $^{\#}p < 0.05$: KH7 + 8-Br-cAMP *vs* KH7; $^{ooo}p < 0.005$: CAI *vs* CTRL; $^{‡}p < 0.05$: CAI + 8-Br-cAMP *vs* CAI. Student's t test. For experimental details see under Materials and methods and legend to Figs. 1 and 2.

like, for example mitochondrial EPAC (cAMP activated guanine nucleotide exchange factors for RAS-like GTPases) [39], are involved in the effects described here. The relationship of the ATP synthase changes with mitochondrial dynamics [40] and apoptosis [29,41] should be the subject of further investigations.

5. Conclusions

In conclusions our study shows that cAMP promotes life essential ATP production by complex V and prevents, at the same time, detour of this complex to a membrane leak conductance involved in cell death.

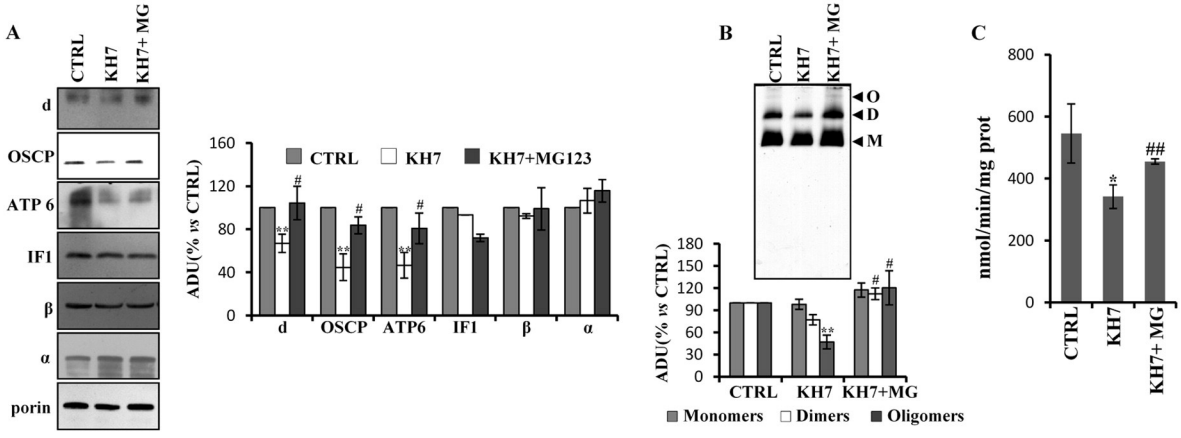

Fig. 7. Effects of KH7 and MG132 on the level of subunits, supramolecular organization and hydrolase activity of the ATP synthase complex in RLM. RLM were treated for 10 min at 30 °C in the absence (CTRL), in the presence of KH7 (KH7) or of 50 μM KH7 plus 10 μM MG132 (KH7 + MG). Panel A, immuno-detection of subunit levels. Panel B, mitochondrial complexes separated by CN-PAGE and gel incubation with ATP and lead nitrate to reveal the ATPase activity. The histograms represent the ADU percentage changes with respect to the ADU of control untreated RLM. Panel C, ATP hydrolase activity in control and treated RLM. The values are means ± standard deviation of determinations in three separate RLM preparations. $^{**}p < 0.01$, $^{*}p < 0.05$: KH7 *vs* CTRL; $^{\#\#}p < 0.01$, $^{\#}p < 0.05$: KH7 + MG132 *vs* KH7. Student's t test.

Competing interests

The authors declare no conflict of interest.

Transparency document

The Transparency document associated with this article can be found, in online version.

Acknowledgments

This work has been supported by a grant to D.D.R. from MIUR (Progetto FIRB futuro in ricerca, 2008) [RBFR0813Z5] and a grant to S.P. from MIUR (FIRB-MERIT 'Molecular basis in ageing-related degenerative syndrome') [RBNE08HWLZ].

References

[1] J.A. Beavo, L.L. Brunton, Cyclic nucleotide research — still expanding after half a century, Nat. Rev. Mol. Cell. Biol. 3 (2002) 710–718.
[2] F. Valsecchi, L.S. Ramos-Espiritu, J. Buck, L.R. Levin, G. Manfredi, cAMP and mitochondria, Physiology (Bethesda) 28 (2013) 199–209.
[3] M.A. Davare, V. Avdonin, D.D. Hall, E.M. Peden, A. Burette, R.J. Weinberg, M.C. Horne, T. Hoshi, J.W. Hell, A beta$_2$ adrenergic receptor signaling complex assembled with the Ca^{2+} channel Cav1.2, Science 293 (2001) 98–101.
[4] Y. Chen, M.J. Cann, T.N. Litvin, V. Iourgenko, M.L. Sinclair, L.R. Levin, J. Buck, Soluble adenylyl cyclase as an evolutionarily conserved bicarbonate sensor, Science 289 (2000) 625–628.
[5] T.N. Litvin, M. Kamenetsky, A. Zarifyan, J. Buck, L.R. Levin, Kinetic properties of "soluble" adenylyl cyclase. Synergism between calcium and bicarbonate, J. Biol. Chem. 278 (2003) 15922–15926.
[6] G. Di Benedetto, E. Scalzotto, M. Mongillo, T. Pozzan, Mitochondrial Ca2 + uptake induces cyclic AMP generation in the matrix and modulates organelle ATP levels, Cell Metab. 17 (2013) 965–975.
[7] J.H. Zippin, Y. Chen, S.G. Straub, K.C. Hess, A. Diaz, D. Lee, P. Tso, G.G. Holz, G.W. Sharp, L.R. Levin, J. Buck, CO_2/$HCO_3^{(-)}$- and calcium-regulated soluble adenylyl cyclase as a physiological ATP sensor, J. Biol. Chem. 288 (2013) 33283–33291.
[8] K. Lefkimmiatis, D. Leronni, A.M. Hofer, The inner and outer compartments of mitochondria are sites of distinct cAMP/PKA signaling dynamics, J. Cell Biol. 202 (2013) 453–462.
[9] A.M. Sardanelli, A. Signorile, R. Nuzzi, D. De Rasmo, Z. Technikova-Dobrova, Z. Drahota, A. Occhiello, A. Pica, S. Papa, Occurrence of A kinase anchor protein and associated cAMP-dependent protein kinase in the inner compartment of mammalian mitochondria, FEBS Lett. 580 (2006) 5690–5696.
[10] S. Papa, A.M. Sardanelli, S. Scacco, Z. Technikova-Dobrova, cAMP-dependent protein kinase and phosphoproteins in mammalian mitochondria. An extension of the cAMP-mediated intracellular signal transduction, FEBS Lett. 444 (1999) 245–249.
[11] S. Papa, A.M. Sardanelli, S. Scacco, V. Petruzzella, Z. Technikova-Dobrova, R. Vergari, A. Signorile, The NADH: ubiquinone oxidoreductase (complex I) of the mammalian respiratory chain and the cAMP cascade, J. Bioenerg. Biomembr. 34 (2002) 1–10.
[12] R. Acin-Perez, E. Salazar, M. Kamenetsky, J. Buck, L.R. Levin, G. Manfredi, Cyclic AMP produced inside mitochondria regulates oxidative phosphorylation, Cell Metab. 9 (2009) 265–276.
[13] S. Papa, D. De Rasmo, Z. Technikova-Dobrova, D. Panelli, A. Signorile, S. Scacco, V. Petruzzella, F. Papa, G. Palmisano, A. Gnoni, L. Micelli, A.M. Sardanelli, Respiratory chain complex I, a main regulatory target of the cAMP/PKA pathway is defective in different human diseases, FEBS Lett. 586 (2012) 568–577.
[14] S. Papa, D. De Rasmo, Complex I deficiencies in neurological disorders, Trends Mol. Med. 19 (2013) 61–69.
[15] J.T. Cribbs, S. Strack, Reversible phosphorylation of Drp1 by cyclic AMP-dependent protein kinase and calcineurin regulates mitochondrial fission and cell death, EMBO Rep. 8 (2007) 939–944.
[16] D. De Rasmo, G. Gattoni, F. Papa, A. Santeramo, C. Pacelli, T. Cocco, L. Micelli, N. Sardaro, M. Larizza, M. Scivetti, S. Milano, A. Signorile, The β-adrenoceptor agonist isoproterenol promotes the activity of respiratory chain complex I and lowers cellular reactive oxygen species in fibroblasts and heart myoblasts, Eur. J. Pharmacol. 652 (2011) 15–22.
[17] R. Acin-Perez, E. Salazar, S. Brosel, H. Yang, E.A. Schon, G. Manfredi, Modulation of mitochondrial protein phosphorylation by soluble adenylyl cyclase ameliorates cytochrome oxidase defects, EMBO Mol. Med. 1 (2009) 392–406.
[18] D. De Rasmo, A. Signorile, A. Santeramo, M. Larizza, P. Lattanzio, G. Capitanio, S. Papa, Intramitochondrial adenylyl cyclase controls the turnover of nuclear-encoded subunits and activity of mammalian complex I of the respiratory chain, Biochim. Biophys. Acta 1853 (2015) 183–191.
[19] S. Papa, P.L. Martino, G. Capitanio, A. Gaballo, D. De Rasmo, A. Signorile, V. Petruzzella, The oxidative phosphorylation system in mammalian mitochondria, Adv. Exp. Med. Biol. 942 (2012) 3–37.
[20] J. Habersetzer, W. Ziani, I. Larrieu, C. Stines-Chaumeil, M.F. Giraud, D. Brèthes, A. Dautant, P. Paumard, ATP synthase oligomerization: from the enzyme models to the mitochondrial morphology, Int. J. Biochem. Cell Biol. 45 (2013) 99–105.
[21] D. Stock, C. Gibbons, I. Arechaga, A.G. Leslie, J.E. Walker, The rotary mechanism of ATP synthase, Curr. Opin. Struct. Biol. 10 (2000) 672–679.
[22] H. Noji, R. Yasuda, M. Yoshida, K.jr. Kinosita, direct observation of the rotation of F1-ATPase, Nature 386 (1997) 299–302.
[23] R.D. Allen, C.C. Schroeder, A.K. Fok, An investigation of mitochondrial inner membranes by rapid-freeze deep-etch techniques, J. Cell Biol. 108 (1989) 2233–2240.
[24] I. Arnold, K. Pfeiffer, W. Neupert, R.A. Stuart, H. Schägger, Yeast mitochondrial F1F0-ATP synthase exists as a dimer: identification of three dimer-specific subunits, EMBO J. 17 (1998) 7170–7178.
[25] I. Wittig, H. Schägger, Supramolecular organization of ATP synthase and respiratory chain in mitochondrial membranes, Biochim. Biophys. Acta 1787 (2009) 672–680.
[26] P. Paumard, J. Vaillier, B. Coulary, J. Schaeffer, V. Soubannier, D.M. Mueller, D. Brèthes, J.P. di Rago, J. Velours, The ATP synthase is involved in generating mitochondrial cristae morphology, EMBO J. 21 (2002) 221–230.
[27] C. Bornhövd, F. Vogel, W. Neupert, A.S. Reichert, Mitochondrial membrane potential is dependent on the oligomeric state of F1F0-ATP synthase supracomplexes, J. Biol. Chem. 281 (2006) 13990–13998.
[28] J. Habersetzer, I. Larrieu, M. Priault, B. Salin, R. Rossignol, D. Brèthes, P. Paumard, Human F1F0 ATP synthase, mitochondrial ultrastructure and OXPHOS impairment: a (super-)complex matter? PLoS One 8 (2013), e75429.
[29] K.N. Alavian, H. Li, L. Collis, L. Bonanni, L. Zeng, S. Sacchetti, E. Lazrove, P. Nabili, B. Flaherty, M. Graham, Y. Chen, S.M. Messerli, M.A. Mariggio, C. Rahner, E. McNay, G.C. Shore, P.J. Smith, J.M. Hardwick, E.A. Jonas, Bcl-xL regulates metabolic efficiency of neurons through interaction with the mitochondrial F1FO ATP synthase, Nat. Cell Biol. 13 (2011) 1224–1233.
[30] M. Bonora, A. Bononi, E. De Marchi, C. Giorgi, M. Lebiedzinska, S. Marchi, S. Patergnani, A. Rimessi, J.M. Suski, A. Wojtala, M.R. Wieckowski, G. Kroemer, L. Galluzzi, P. Pinton, Role of the c subunit of the FO ATP synthase in mitochondrial permeability transition, Cell Cycle 12 (2013) 674–683.
[31] K.N. Alavian, G. Beutner, E. Lazrove, S. Sacchetti, H.A. Park, P. Licznerski, H. Li, P. Nabili, K. Hockensmith, M. Graham, G.A. Jr Porter, E.A. Jonas, An uncoupling channel within the c-subunit ring of the F1FO ATP synthase is the mitochondrial permeability transition pore, Proc. Natl. Acad. Sci. U. S. A. 111 (2014) 10580–10585.
[32] P. Bernardi, F. Di Lisa, F. Fogolari, G. Lippe, From ATP to PTP and back: a dual function for the mitochondrial ATP synthase, Circ. Res. 116 (2015) 1850–1862.
[33] A. Ito, T. Ogishima, W. Ou, T. Omura, H. Aoyagi, S. Lee, H. Mihara, N. Izumiya, Effects of synthetic model peptides resembling the extension peptides of mitochondrial enzyme precursors on import of the precursors into mitochondria, J. Biochem. 98 (1985) 1571–1582.
[34] I. Wittig, H.-P. Braun, H. Schagger, Blue native PAGE, Nat. Protoc. 1 (2006) 418–428.
[35] E. Zerbetto, L. Vergani, F. Dabbeni-Sala, Quantification of muscle mitochondrial oxidative phosphorylation enzymes via histochemical staining of blue native polyacrylamide gels, Electrophoresis 18 (1997) 2059–2064.
[36] E.R. Swenson, New insights into carbonic anhydrase inhibition, vasodilation, and treatment of hypertensive-related diseases, Curr. Hypertens. Rep. 16 (2014) 467.
[37] S. Srinivasan, J. Spear, K. Chandran, J. Joseph, B. Kalyanaraman, N.G. Avadhani, Oxidative stress induced mitochondrial protein kinase A mediates cytochrome C oxidase dysfunction, PLoS One 8 (2013), e77129.
[38] F. Valsecchi, C. Konrad, G. Manfredi, Role of soluble adenylyl cyclase in mitochondria, Biochim. Biophys. Acta 1842 (2014) 2555–2560.
[39] S.S. Roscioni, C.R. Elzinga, M. Schmidt, Epac: effectors and biological functions, Naunyn Schmiedeberg's Arch. Pharmacol. 377 (2008) 345–357.
[40] G.M. Cereghetti, A. Stangherlin, O. Martins de Brito, C.R. Chang, C. Blackstone, P. Bernardi, L. Scorrano, Dephosphorylation by calcineurin regulates translocation of Drp1 to mitochondria, Proc. Natl. Acad. Sci. U. S. A. 105 (2008) 15803–15808.
[41] N.N. Danial, BAD: undertaker by night, candyman by day, Oncogene 27 (Suppl. 1) (2008) S53–S70.